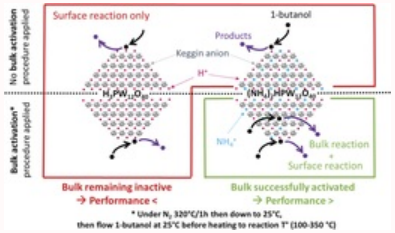

Ammonium-substitution for successfully activating the bulk of Keggin acid salts in 1-butanol dehydration[†]

[†]Electronic supplementary information (ESI) available. See DOI: 10.1039/d0cy00820f

Charlotte Lang,[a] ORCID: 0000-0003-3352-8058

Josefine Schnee,[b] ORCID: 0000-0001-8521-9922

Boris Junior Takam Mba,[a]

François Devred,[a] ORCID: 0000-0002-3342-5393

Eric M. Gaigneaux[*,a] ORCID: 0000-0003-2239-4306

[a]Université catholique de Louvain, Institute of Condensed Matter and Nanosciences, Place Louis Pasteur 1 box L4.01.09, B-1348 Louvain-la-Neuve, Belgium. Email: eric.gaigneaux@uclouvain.be

[b]ENSICAEN, UNICAEN, CNRS, Laboratoire Catalyse et Spectrochimie, Normandie Université, Boulevard Maréchal Juin 6, F-14050 Caen, France.

Abstract

In 1-butanol dehydration (gas phase) on a Keggin heteropolyacid (HPA) catalyst, the large size of 1-butanol and its significant hydrophobicity make the bulk-type (also called pseudo liquid-type) catalytic mechanism impossible. This drastically limits the catalytic effect on the surface of the HPA, with an activity lower than what it could be. To overcome this limitation, partially substituted ammonium Keggin acid salts with the formula $(NH_4)_xH_{3-x}PW_{12}O_{40}$ were here synthesized. Still maintaining enough acidity for the dehydration reaction, the replacement of some protons of $H_3PW_{12}O_{40}$ with NH_4^+ increases the hydrophobicity of the crystal matrix and allows 1-butanol to enter the bulk of the salt. This consequently makes the protons inside the solid able to catalyse the reaction. The penetration of 1-butanol in the bulk is demonstrated by a combination of *in situ* methods (Raman, FTIR and XRD) applied during the pre-treatment of the catalyst and the catalytic reaction. When properly activated the pseudo liquid-type mechanism taking place in $(NH_4)_xH_{3-x}PW_{12}O_{40}$ leads to a markedly higher 1-butanol conversion in comparison to the surface-type mechanism which is the only one achieved with the non-modified pristine HPA.

1. Introduction

Nowadays, it is very important to develop new routes for biomass valorisation in order to replace oil derivatives as starting materials for production of fuels, polymers and other fine chemicals. One way is to

produce alcohols by biomass fermentation, which can then be transformed through a dehydration route to molecules that are useful for the chemical industry.[1] The use of methanol in such dehydration leads to dimethyl ether as the only product (eqn (1)),[2,3] but the use of longer alcohols can lead to a wider range of molecules that includes next to ethers (eqn (1)) unsaturated compounds (eqn (2)).[4]

$$2R\text{-}CH_2\text{-}OH \rightarrow R\text{-}CH_2\text{-}O\text{-}CH_2\text{-}R + H_2O \quad (\mathbf{1})$$

$$R\text{-}CH_2\text{-}OH \rightarrow R = CH_2 + H_2O \quad (\mathbf{2})$$

In this study, 1-butanol dehydration is explored, looking at the formation of dibutylether but also 1-butene, *trans*-2-butene and *cis*-2-butene.

In general, dehydration reactions are achieved with strongly acidic liquid catalysts as concentrated sulphuric acid. However, it is possible to use some heterogeneous solid acid catalysts that are less toxic, and much safer to handle. Such kind of solid catalysts, like aluminas or silica-aluminas,[5,6] zeolites[1,5,7] or heteropolyacids,[2,3,8–10] can be used in continuous processes working with a gaseous reagent passing through the solid catalyst bed.

Specifically heteropolyacids are nowadays largely used for many kinds of reactions, thanks to their oxidative properties under mild conditions, and their simultaneous very strong acidity approaching superacidity.[9,11,12] Among their wide variety of structures, Keggin type is the most common one thanks to its high stability compared to other structures.[11–14] The Keggin anion $[XM_{12}O_{40}]^{n-}$ is composed of a central XO_4 tetrahedron containing the heteroatom X (typically P^{5+}, Si^{4+}, *etc.*) and surrounded by twelve MO_6 octahedra containing the addenda atom M (typically W^{6+}, Mo^{6+}, *etc.*).[9,11,12,15] Keggin anions crystallize with protons to form $H_nXM_{12}O_{40}$ heteropolyacids, the most stable and acidic one being $H_3PW_{12}O_{40}$.

One important peculiarity of heteropolyacids is their ability to achieve a pseudo liquid phase type catalytic mechanism inside their bulk.[2,12,16,17] The bulk is represented by the spaces between the Keggin anions in the crystalline structure. The access of the reactant molecules to the bulk is a major advantage as, although such diffusion of the reactant molecules towards and through the bulk might be slow, it allows benefitting from the catalytic potential of every single proton present inside the catalyst. In other words it adds more active sites in the catalytic game and allows the reaction to proceed with more than the only protons present at the surface of the catalyst as when the reaction only follows a classical surface-type mechanism. It is thus of utmost importance to develop strategies to properly activate the catalysts in order to bring substrate molecules to react inside their bulk.

Schnee *et al.* showed that submitting solid $H_3PW_{12}O_{40}$ to proper conditions it is possible to replace its crystallization water by methanol, which corresponds to the activation of its bulk and allows the conversion of methanol inside it during the subsequent catalytic reaction.[2,18] This activation is possible with methanol because it is a small and hydrophilic molecule. In the case of longer aliphatic alcohols however, like 1-butanol, succeeding such activation is more difficult, because of their bigger size and higher hydrophobicity.[19,20] The difficulties of 1-butanol to penetrate the bulk of HPA, in comparison to methanol and other small polar molecules, are discussed in the literature.[16,21] To overcome this problem, we directed our strategy to the modification of Keggin heteropolyacids with cations that would make their bulk more accessible to bigger and more hydrophobic molecules. The idea is precisely to create a homogeneous $Z_xH_{n-x}XM_{12}O_{40}$ phase, which contains simultaneously protons and bigger cations (generally noted as Z at this stage); the hypothesis being that such substitution will increase the lattice parameter of the cubic phase as described by Vegard,[22] with accordingly the creation of more space for 1-butanol to penetrate in the bulk. Another facet of our hypothesis is that all substitutions leading to an increase of the hydrophobicity of the Keggin salt matrix (as should be the case when replacing hydrophilic, and usually hydrated, protons) would help more hydrophobic molecules to have more interactions with the catalyst and penetrate its bulk.

It is possible to substitute some protons of $H_nXM_{12}O_{40}$ heteropolyacid by cations like Na^+, Cs^+, NH_4^+ or Ag^+.[16,17] We decided to study partially substituted ammonium Keggin heteropolyoxometalate acid salts.[17,23,24] These catalysts are claimed to have higher specific surface area and/or microporosity than those of the corresponding pristine heteropolyacids.[17,24] Substitution of protons with ammonium cations should lead to a modification of their lattice parameter, but it will also decrease the number of acid sites, *i.e.* with fewer remaining protons to catalyze the reaction. In the scope of our strategy to optimize these catalysts for acid-driven dehydration reactions, it is thus crucial to succeed in achieving only partial substitution of pristine protons so as to preserve significant acidity for the catalysis. Finding synthesis conditions leading to a good compromise between the modification of the solid properties, and the number and acid strength of the protons still available for the reaction is the core of the investigation reported here. After the synthesis of the modified Keggin salts and their *ex situ* characterization, a combination of *in situ* techniques (Raman, FTIR and X-ray diffraction) are implemented to elucidate the phenomenon occurring during the activation and reaction of the catalysts. Specifically these techniques are used to follow the penetration of 1-butanol in the bulk of the substituted salts and decipher which catalytic mechanism (surface-type or pseudo liquid one) does operate with our catalysts.[2,25]

2. Experimental

2.1. Chemicals

All chemicals were purchased from Roth. Before use, $H_3PW_{12}O_{40}$ (hereafter H3PW) was dried under vacuum at 25 °C overnight in order to remove physisorbed water. NH_4HCO_3 and 1-butanol reagent grade (≥99.5%) were used as received.

2.2. Materials preparation

$(NH_4)_xH_{3-x}PW_{12}O_{40}$ catalysts (hereafter denoted as $(NH_4)x$PW) were prepared as follows. First, a NH_4HCO_3 aqueous solution (0.025 mol L^{-1}) was added dropwise (room temperature, under stirring) to a $H_3PW_{12}O_{40}$ aqueous solution (0.055 mol L^{-1}) in determined proportions to obtain the desired x.[23] A solid precipitated progressively. The obtained suspension was aged for 1 night at ambient temperature in atmospheric air in a covered flask. Then, the suspension was slowly dried at 50 °C under vacuum in a rotary evaporator. The obtained powders were finally heated at 150 °C for 8 hours in an oven in air, in order to homogenise them.[17] Catalysts $(NH_4)x$PW were prepared with x = 0.5, 1, 1.5, 2, 2.5 and 3.

2.3. *Ex situ* characterisation

X-ray diffraction (XRD) patterns were acquired at room temperature with a D8 ADVANCE Bruker diffractometer equipped with a LYNXEYE XE-T detector, using copper Kα radiation (λ = 0.15418 nm) in a 2θ range of 5–80° (step = 0.015°, time per step = 0.15 s). The X-ray source was operated with a tension of 40 kV and a current of 30 mA. The powder diffraction file from the International Center for Diffraction Data (PDF-2 database, ICDD[26]) was used to identify the crystalline phases and DIFFRAC-EVA was used for data analysis. The lattice parameters were calculated using eqn (3).

$$a = d \times \sqrt{h^2 + k^2 + l^2}, \quad (3)$$

where a is the lattice parameter in Å, d is the basal distance in Å, and h, k and l are the indexes from the literature (pdf-2 50-0304) relative to each peak used.

Thermogravimetric analysis (TGA) was performed using a Mettler Toledo TGA/SDTA851. The sample (around 15 mg) was heated under a dry air stream (Air Liquide Alphagaz 1 dry air 99.9%, 50 mL min^{-1}) from room temperature to 800 °C, 10 °C min^{-1}, in order to evaluate the amount of physisorbed and structural water, and the decomposition temperature of the Keggin salts.

NH_3 temperature programmed desorption (NH_3-TPD) was performed using a Hiden CATLAB-PCS combined microreactor and mass spectrometer (MS) system. The MS was equipped with a quadrupole detector. In the first step, the sample (around 50 mg) was heated under argon (30 mL min^{-1}, Air Liquide purity Alphagaz 1 = 99.999%) at 150 °C. Then, the sample was exposed to ammonia (Praxair certified gas mixture 5% NH_3 in He (Alphagaz 1 = 99.999%) 10 mL min^{-1} diluted with Ar 20 mL min^{-1}) for 2 hours at 150 °C and then flushed with Ar (30 mL min^{-1}) for 1.5 h to remove physisorbed ammonia. The last step consisted in the desorption of chemisorbed ammonia, by increasing the temperature from 150 °C to 700 °C at the rate of 10 °C min^{-1}. As the catalyst contains ammonium, the same procedure was applied without flowing ammonia during the adsorption step, namely flowing 30 mL min^{-1} of only argon for 2 h at 150 °C, in order to quantify the number of ammonia molecules corresponding to the ammonium structurally present in the catalyst. The difference between these two measurements (with and without ammonia adsorption) gives the number of ammonia molecules just related to the acid sites in the catalyst and is called “corrected ammonia molecules”. Only corrected values are presented below. The ammonia mass signal (mz17) is also corrected by removing the contribution of H_2O at the same mass, which was estimated from the H_2O signal measured at the mass signal (mz18). Sensitivity factors were calculated based on the first step of ammonia adsorption and used to calibrate and quantify the amount of released ammonia.

2.4. *In situ* characterization

Catalysts were characterized by *in situ* Raman spectroscopy during the bulk activation procedure (dehydration and then 1-butanol exposure, see later). The sample (180 mg) was introduced into a quartz reactor, equipped with optical windows allowing the characterization by Raman spectroscopy during the procedure. The reactor was connected to gas flowmeters and a 1-butanol saturator in order to control the gas composition, and inserted in a tubular furnace in order to control the temperature. A hole drilled in the furnace allowed the laser to be focused on the sample to irradiate it and to collect its Raman signal. The whole setup was placed within a black box in order to avoid any disturbances from external lights. Raman spectra were recorded with a Kaiser RXN spectrometer (diode-pumped frequency doubled Nd:YAG 1 laser with 532 nm wavelength, a nominal power of 50 mW, an Mk II filtered probe head with a 5.5 inch non-contact objective lens, and a spot-size of *ca.* 100 μm). The resolution was 5 cm^{-1}. The spectrometer had an objective through which the laser beam was focused at a distance of about 14 cm. The acquisition consisted of 15 accumulations of 1 second exposure for each spectrum, with 2 minutes between two spectra.

Catalysts were characterized by *in situ* FT-IR spectroscopy upon dehydration and subsequent exposure to 1-butanol. Each of the samples (5 mg) was dispersed in deionized water and spread over a silicon plate (2 cm^2 area).

After 5 minutes of drying in ambient air, the silicon plate was placed in a homemade transmission IR cell, which in turn was positioned in the sample compartment of a Thermo-Nicolet Nexus 670 FT-IR spectrometer. The IR cell was equipped with IR-transparent KBr windows at each side of the sample holder, and with a heating system. It was connected to a vacuum line for evacuation (to 10^{-6} Torr) and subsequent introduction of small doses of 1-butanol vapor (typically 1.5 Torr). The spectrometer was equipped with a mercury cadmium telluride (MCT) cryo-detector. *In situ* FT-IR spectra during evacuation and butanol-exposure steps were measured at 4 cm^{-1} resolution, and processed with the Thermo Scientific OMNIC software. In a typical experiment, the sample was first pre-treated under vacuum (10^{-6} Torr) according to the following steps: 1) 30 minutes at room temperature, 2) heating to 320 °C (8 °C min^{-1}) for 1 hour, and 3) cooling down to 150 °C (8 °C min^{-1}). Once at 150 °C, the sample is exposed to 1.5 Torr of 1-butanol (Sigma-Aldrich, ≥99%). Then, it was kept under the latter atmosphere for the whole 3 following steps: 1) 10 minutes at 150 °C, 2) cooling down to room temperature (10 °C min^{-1}) for 1 night, 3) heating back to 150 °C (2 °C min^{-1}) for 1 hour, and 4) cooling down again to room temperature (10 °C min^{-1}). Finally, once back at room temperature, 1-butanol was evacuated (until reaching 10^{-6} Torr).

X-ray diffraction patterns were acquired on the same apparatus as described before, but with the catalytic chamber (Bruker XRK900) mounted on the diffractometer. X-ray diffractograms were continuously recorded throughout the bulk activation procedure (dehydration and subsequent exposure to 1-butanol). For this, the gas was flushed in the chamber at a flow of 30 mL min^{-1} and atmospheric pressure, at a temperature and with the gas composition following exactly the sequence described in section 2.5.

2.5. Catalytic activity

The catalysts were tested in 1-butanol dehydration between 100 and 350 °C. The N_2 (Air Liquide Alphagaz 1 = 99.999%) flow was controlled using a N_2 mass flowmeter and sent to a saturator filled with 1-butanol. The temperature of the saturator (64.6 °C)[27] leads to a 1-butanol partial pressure of 10% in the mixture (total flow 30 mL min^{-1}). All the gas lines of the setup were heated at around 200 °C to avoid any condensation. The catalysts (0.180 g of powders as prepared but selected by sieving in a granulometer between 100 and 200 μm after an eventual slight mortar-and-pestle crushing, catalytic bed of 2.0 cm) were tested in a stainless steel tubular reactor heated in a furnace.

In the case where the activation step of the bulk was applied, the catalyst was first treated at 320 °C for 1 h under N_2 in order to remove all the physisorbed and structural water.[2] Then, the temperature was decreased to 25 °C and when 25 °C was reached the catalyst was exposed to 1-butanol (partial pressure 1%) for 10 minutes. After that, it was flushed with nitrogen and the catalytic test started. This temperature and exposure sequence was the one described in ref. 2 to allow methanol to penetrate in the bulk of HPW, here replacing methanol by 1-butanol. These tests are labelled “1-butanol exposure”.

When no such activation procedure was applied, the catalyst was only treated at 320 °C for 1 h under N_2 in order to remove all the physisorbed and structural water, then the temperature was decreased to 100 °C and when 100 °C was reached the catalytic test started by introducing the mixture 1-butanol/N_2 in the reactor. These tests are labelled “no exposure”.

Outlet products were analysed online using a 450-gas chromatograph from Bruker, equipped with a molecular sieve 5 Å column (separation of N_2 and CO) followed by a TCD, a pre-packed column HAYESEP Q 80–100 (separation of CO_2) followed by a TCD and a capillary SIL-5CB column followed by a FID for the separation and detection of organic compounds (butenes, 1-butanol, dibutylether and heavier compounds).

Catalytic results are given in terms of 1-butanol conversion (%C_{BuOH}) (eqn (4)), butenes and dibutylether (DBE) selectivities (%$S_{1\text{-butene}}$, %$S_{t\text{-2-butene}}$, %$S_{c\text{-2-butene}}$, %S_{DBE},) (eqn (5)) and carbon balance (%CB) (eqn (6)). Moreover to evaluate and properly compare the intrinsic performance of the different catalysts, a normalized conversion has been calculated per acid site present in the reactor. The number of acid sites per mass of the different catalysts was evaluated by NH_3-TPD (*vide supra*). All the catalysts being tested at the same mass and under identical flow conditions, the differences between them at the level of their normalized conversions are a direct reflection of their differences in intrinsic reaction rates.

$$\%C_{BuOH} = \frac{BuOH_{in} - BuOH_{out}}{BuOH_{in}} \times 100, \quad (4)$$

where $BuOH_{in}$ and $BuOH_{out}$ are percentages of 1-butanol respectively at the inlet and at the outlet.

$$\%S_x = \frac{\%Y_x}{\%C_{BuOH}} \times 100, \quad (5)$$

where $\%S_x$ is the selectivity of compound *X*.

$$\%CB = \frac{Butenes_{out} + 2 \times DBE_{out} + BuOH_{out}}{BuOH_{in}} \times 100, \quad (6)$$

where %CB is the carbon balance.

The aim of the work is to demonstrate when the catalysts are active according to a pseudo liquid reaction mechanism, *i.e.* when the substrate penetrates inside the bulk and reacts with the protons therein in addition to the reaction it undergoes with the protons present at the surface of the catalysts. In this context, calculating rates (number of 1-butanol molecules converted, per active site, per time unit) would not be helpful. Indeed, in the case we succeed to make the reaction occuring not only at the surface but also in the bulk (as we target it), internal diffusion of 1-butanol inside the bulk of the salts likely comes into play and might decrease, (as it might indeed be a slow step), the overall reaction rates. This would make unfair the comparison of on one side the rates when the pseudo liquid mechanism is active, with on the other side rates resulting of an exclusively surface-type reaction mechanism (as would be systematically lost by the catalysts achieving the pseudo liquid mechanism. The aim here is to increase the number of catalytic sites contributing to the reaction (by activating the bulk protons in addition to the surface ones), whether their rates are slowed down by the diffusion (inner protons) or not (surface protons). This approach was already validated in ref. 2.

3. Results and discussion

3.1. *Ex situ* characterization of the prepared partially substituted ammonium Keggin acid salts

3.1.1. X-ray diffraction

X-ray diffraction analysis (Fig. 1) revealed the presence of a $(NH_4)_xPW$ phase from $x = 0.5$ to $x = 3$, and the presence of a H3PW phase from $x = 0$ to $x = 1.5$. The presence of two phases for samples with $0 < x \leq 1.5$ indicates a certain inhomogeneity in them. According to the literature, during the preparation of the catalysts, the precipitation of $(NH_4)_xPW$ particles with a real x higher than the nominal one likely occurs first, then with the evaporation of the solvent, the rest of HPA still in solution deposits on the first-formed $(NH_4)_xPW$ particles.[17] Also according to the literature, the subsequent thermal treatment is intended to homogenize the system by allowing a migration of the different cations and their equilibration throughout the whole solid,[17] but for the samples with low x, our results suggest that the H3PW layer deposited over $(NH_4)_xPW$ particles is likely too thick and such homogenization becomes difficult, leading at the end to a mixture of $(NH_4)_xPW$ and H3PW.

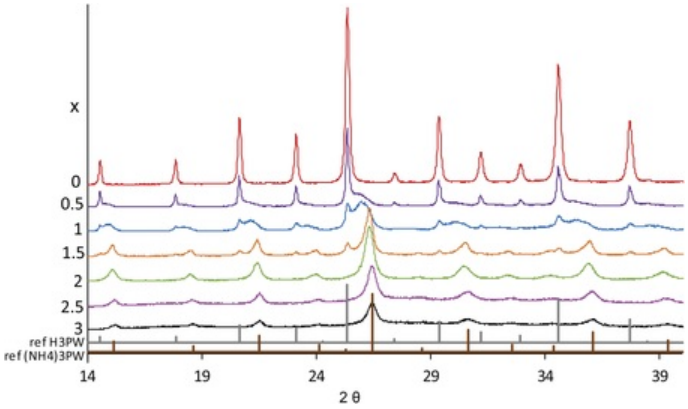

Fig. 1 X-ray diffraction, – H3PW, – $(NH_4)0.5PW$, – $(NH_4)1PW$, – $(NH_4)1.5PW$, – $(NH_4)2PW$, – $(NH_4)2.5PW$, – $(NH_4)3PW$, – ref $H_3PW_{12}O_{40}{\cdot}6H_2O$ ICDD 2004 pdf-2 50-0304, – ref $(NH_4)_3PW_{12}O_{40}{\cdot}9.5H_2O$ ICDD 2004 pdf-2 50-0305.

The H3PW phase disappeared progressively when increasing x up to $x = 2$. Above this value, XRD did not detect the presence of the H3PW phase anymore, meaning that the samples with $x \geq 2$ were composed of only the homogeneous partially substituted-phase.

The lattice parameters (Fig. 2) show that an increase in x has no impact on the H3PW phase (when present, *i.e.* when $x < 2$). In contrast, the lattice parameter of the $(NH_4)_xPW$ phase decreased gradually with the increase of x, indicating a progressive insertion of NH_4^+ in the lattice. The decrease in the lattice parameter seems to contradict the idea that introducing a bigger cation (NH_4^+ is indeed bigger than H^+) in the bulk would increase the lattice size. But our observation actually can be related to the loss of structural water, which is present when H^+ is the counter-cation of the polyoxometalate (forming $H_5O_2^+$) but absent with other cations. When crystalline water is removed from pristine HPA, the global crystallinity is affected and the cubic centred structure is lost.[28] The presence of ammonium species here leads to a structure with a low content in crystalline water, still with the pristine crystalline symmetry preserved. This could help 1-butanol to penetrate the bulk, notwithstanding the smaller lattice parameters, because the crystal lattice is not cluttered with water anymore.

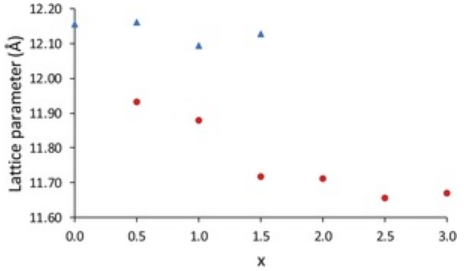

Fig. 2 Lattice parameters of the phases ▲ H3PW and ● $(NH_4)_xPW$, as a function of *x*.

3.1.2. TGA

Based on the TGA profiles, the amounts of physisorbed and structural water were calculated. The comparison of the amount of structural water per Keggin unit as a function of *x* (Fig. 3) shows that the presence of NH_4^+ leads to its huge decrease. In principle for H3PW each proton is solvated by two water molecules, leading to six water molecules per Keggin unit (each holding three protons). By replacing protons with *x* ammonium, we expect the presence of two water molecules per remaining proton, so (6–2*x*) water molecules per Keggin unit. The overall observed tendency is that the amount of structural water in the samples indeed decreases when the substitution of the protons is pushed further (*i.e.* when *x* value increases). This fits well with the decrease in the lattice parameters highlighted by XRD, which also suggests a loss of structural water along the substitution.

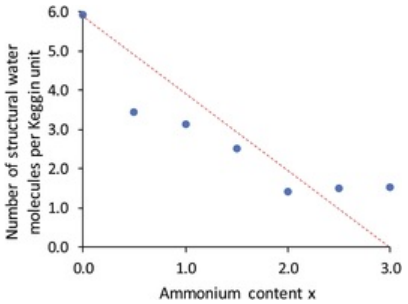

Fig. 3 Number of structural water molecules per Keggin unit as a function of the ammonium content *x* in $(NH_4)_xH_{3-x}PW_{12}O_{40}$. The red dashed line represents the amount of structural water expected from the (6–2*x*) formula, namely 2 water molecules should be present per remaining proton in the structure (*i.e.* not having been substituted by NH_4^+).

Looking more closely, for the samples with $x = 2.5$ and 3, the number of water molecules remains constant, at a slightly higher value than the (6–2*x*) molecules of structural water prediction, suggesting that for very high NH_4^+ contents water remains present in the structure more than expected. This is also correlated with XRD, from which the stabilization of the lattice parameters (no further decrease with *x*) for $x = 2.5$ and $x = 3$ was observed. In contrast an additional fact is that for the lowest *x* (up to $x = 2$), the number of water molecules measured is lower than the (6–2*x*) molecules of structural water prediction. The lower amount of water than expected for these samples with a low *x* value (but different from 0) constitutes a very positive point for the catalytic reaction, as it suggests that the NH_4^+ containing partially substituted structures are likely even less hydrophilic (*i.e.* more hydrophobic) than expected and that they could interact therefore even more easily with 1-butanol.

3.1.3. NH_3-TPD

The ammonia temperature programmed desorption allows quantification of the number of acid sites (number of ammonia molecules desorbed) and their strength (desorption temperature of ammonia) for our samples. It should be noted that the number of acid sites is reported after subtraction of the structural ammonia, *i.e.* present in the crystal structure even before NH_3 adsorption (and thus not probing acid sites) but yet released in the TPD experiment. Fig. 4 shows a decrease in the number of acid sites when *x* increases. The decreasing trend observed confirms that, as expected, H^+ are progressively replaced by NH_4^+ in the crystals when *x* increases.

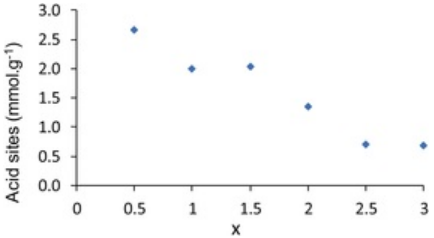

Fig. 4 Number of acid sites in mmol g^{-1} as a function of the ammonium content (x) in $(NH_4)_xH_{3-x}PW_{12}O_{40}$.

For HPA, it is commonly accepted that the acidity brought by protons is so strong that NH_3 is released only when the thermal decomposition of the HPA (or actually of the ammonium salt that is formed when the HPA is exposed to ammonia during the adsorption step of the TPD protocol) occurs.[29,30] This can indeed be observed in Fig. 5 which reveals that H3PW released NH_3, *i.e.* decomposes, at around 600 °C. When implementing ammonium in the structure (*i.e.* substituting H^+), this sign of strong acidity remained predominant for the samples with x = 0.5 to x = 2, even if the stability of the compounds (or their salts formed during the ammonia adsorption step) decreased as their thermal decomposition was observed around 540 °C. When $x \geq 2.5$, almost no sign of strong acidity (x = 2.5) or no strong acidity (x = 3) was observed anymore whereas release of ammonia at a temperature as low as around 260 °C predominated. This release of NH_3 at low temperature could be related either to, first, the presence of weak acid sites as due to the slightly acidic NH_4^+ ions that are present in large quantities for samples with $x \geq 2.5$, or second, to the acidity of the few remaining protons solvated with a proportionally high (actually higher than expected) amount of structural water (as revealed by TGA) that lowered their acid strength. This second hypothesis sounds however unlikely as $(NH_4)_3PW$ shows the strongest NH_3 release at 260 °C while it is not supposed to contain H^+ counter-cation in its structure anymore. A third hypothesis accounting for the low temperature release of ammonia by the samples with the highest x values could be the one used by Essayem *et al.*,[30] namely that ammonium salts of Keggin HPAs become microporous, with the low temperature release of ammonia corresponding to ammonia that had been trapped and somehow stabilized in the small pores during the adsorption step of the TPD protocol, thus without really probing any acid sites during the experiment.

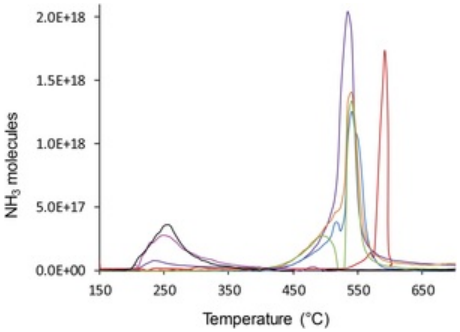

Fig. 5 Number of NH_3 molecules desorbed as a function of the temperature for the samples – H3PW, – (NH_4)0.5PW, – (NH_4)1PW, – (NH_4)1.5PW, – (NH_4)2PW, – (NH_4)2.5PW and – (NH_4)3PW.

3.2. *In situ* characterization of the penetration of 1-butanol in the bulk during the activation procedure

In situ techniques are the easiest way to elucidate whether we succeed in activating the bulk (or not) from one sample to another. It can indeed help to decipher whether the reactant really penetrates the structure and interacts with H^+ ions that are inside the catalyst and not only with those at its surface. The *in situ* characterization was focused only on H3PW, (NH_4)2PW and (NH_4)2.5PW because the *ex situ* characterization confirmed both their homogeneity and remaining acidity. A particular focus was on (NH_4)2PW as this sample was additionally highlighted from the TGA analysis as a more hydrophobic sample than expected, which qualified it as very promising for the catalytic reaction envisaged in our investigation.

3.2.1. H3PW

In situ Raman spectroscopy was first used on H3PW to monitor the effect of the bulk activation procedure on the W═O_t (W═O terminal) band (Fig. 6). It appears that the thermal treatment led to a shift of this band from 1008 cm^{-1} (interaction with dihydrated proton $H_5O_2^+$, Fig. 6a) to 1023 cm^{-1} (corresponding to W═O_t interacting only with anhydrous H^+, Fig. 6b).[2] In the second step, the decrease in the temperature (back to 25 °C) did not lead to a shift of the band back to its initial position, showing that W═O_t remains in interaction with anhydrous H^+ (Fig. 6c). Finally, 1-butanol exposure did not affect the position of the W═O_t band neither (Fig. 6d), indicating that 1-butanol cannot penetrate the bulk and cannot interact with H^+ and/or W═O_t.

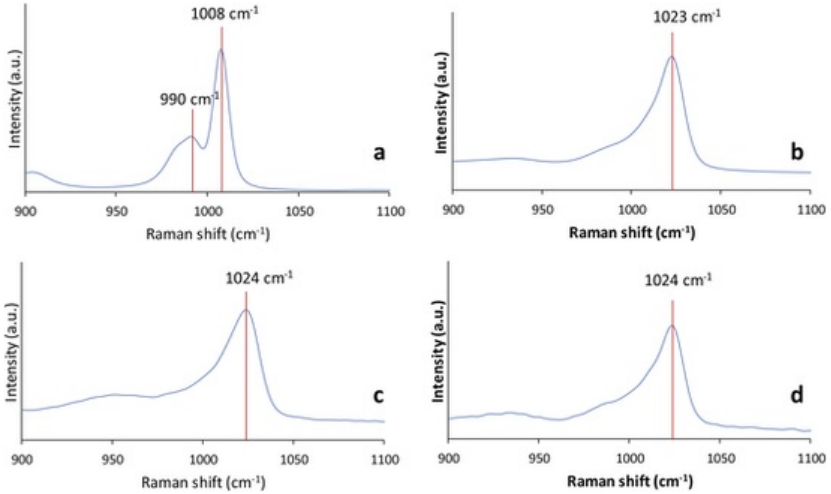

Fig. 6 Raman spectra of H3PW during the bulk activation procedure: a) at 25 °C under N_2, b) at 320 °C under N_2, c) back to 25 °C after thermal treatment under N_2, d) at 25 °C after thermal treatment under 1% 1-butanol in N_2.

The bulk activation procedure was also monitored using XRD. An increase of temperature from 25 °C to 350 °C under a N_2 atmosphere led to the modification of the centred cubic phase to another crystalline phase with less symmetry (Fig. 7). The duration of thermal treatment (0–1 h) did not affect the crystalline phase, and the decrease in the temperature back to 25 °C did not lead to the recovery of the initial centred cubic phase. This evolution of the crystalline phase is due to the loss of structural water when increasing the temperature.

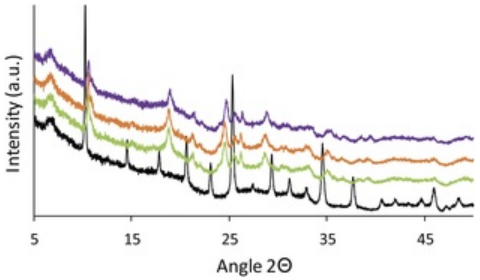

Fig. 7 Evolution of the XRD pattern of H3PW during the thermal treatment of the bulk activation procedure: – start 25 °C, – 350 °C, – 1 h 350 °C, – back to 25 °C.

After the thermal treatment, when H3PW was exposed to 1-butanol no evolution of the crystalline phase was observed neither during the 10 min exposure nor during the N_2 purge (Fig. 8). This confirms that 1-butanol is not able to diffuse within the bulk of H3PW, in good agreement with *in situ* Raman measurements.

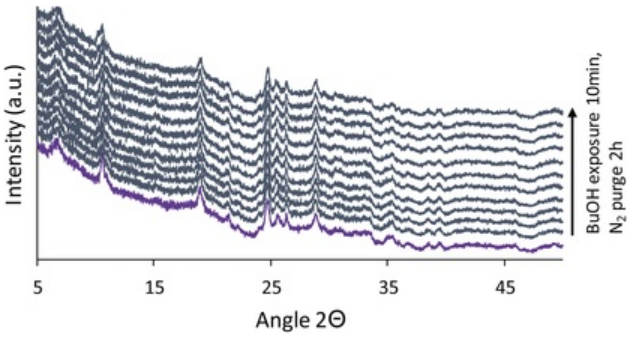

Fig. 8 Evolution of the XRD pattern of H3PW during 1-butanol exposure during the bulk activation procedure: – back to 25 °C (after thermal treatment), – BuOH exposure at 25 °C for 10 min and N_2 purge for 2 h.

Finally, besides bands corresponding to P–Oa–W (1080 cm^{-1}), W–Ob–W (901 cm^{-1}) and W–Oc–W (799 cm^{-1}) that remain unchanged throughout the procedure, *in situ* FT-IR showed that the thermal treatment led to a shift of the W═O_t band from 980 cm^{-1} to 997 cm^{-1} (Fig. 9). This is in good agreement with previous *in situ* studies and the fact that structural water left the structure. However, here the exposure to 1-butanol at 19.8 °C led to the recovery of the initial position of the W═O_t band (from 980 cm^{-1} to 993 cm^{-1}), indicating that something penetrates the bulk and interacts with H^+ and/or W═O_t.

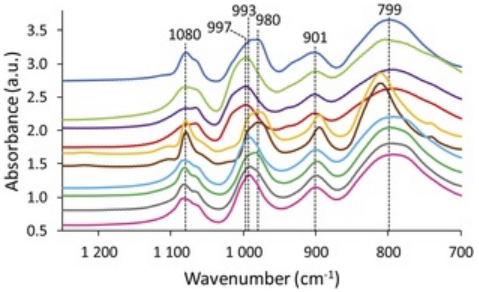

Fig. 9 Evolution of the IR spectrum of H3PW during the bulk activation procedure between 700 and 1400 cm^{-1}: – vacuum 21.5 °C, – vacuum 320 °C, – vacuum 114 °C, – BuOH 1.5 Torr 134 °C, – BuOH 1.5 Torr room temperature, – BuOH 1.5 Torr 19.8 °C, – BuOH 1.5 Torr 140 °C, – BuOH 1.5 Torr 32 °C, – vacuum 25 °C, – vacuum 113 °C.

Scrutinizing this observation on the basis of the spectra at higher wavenumbers (Fig. 10) some water bending was observed around 1615–1620 cm^{-1}, even after 1-butanol exposure, meaning that the 1-butanol used contained traces of water that had interacted with the sample during 1-butanol exposure. Consequently, the observed shift of the W═O_t band is not sufficient to conclude on the efficiency of the bulk activation procedure and its efficiency to allow 1-butanol to infiltrate the bulk of H3PW.

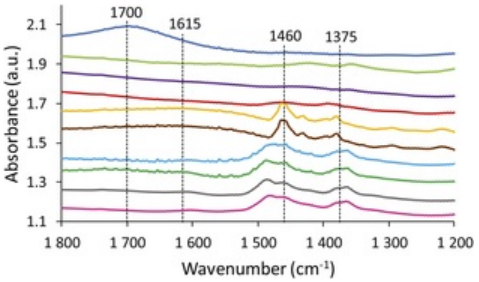

Fig. 10 Evolution of the IR spectrum of H3PW during the bulk activation procedure between 1200 and 1800 cm^{-1}: – vacuum 21.5 °C, – vacuum 320 °C, – vacuum 114 °C, – BuOH 1.5 Torr 134 °C, – BuOH 1.5 Torr room temperature, – BuOH 1.5 Torr 19.8 °C, – BuOH 1.5 Torr 140 °C, – BuOH 1.5 Torr 32 °C, – vacuum 25 °C, – vacuum 113 °C.

Concerning the evolution of the H3PW IR spectrum between 2500 and 4000 cm^{-1} during the bulk activation procedure, we cannot see any formal evidence of 1-butanol entering the bulk (see ESI,† Fig. SI1).

3.2.2. (NH4)2PW

The *in situ* Raman study revealed that during the bulk activation procedure only some W═O_t groups of $(NH_4)2PW$ shifted from 1006 cm^{-1} (Fig. 11a) to a higher value (Fig. 11b). This resulted in a major band at 1005 cm^{-1} (W═O_t that remains in interaction with NH_4^+) and a shoulder at 1018 cm^{-1} (W═O_t interacting with H^+ that has lost its structural water during the thermal treatment). The decrease in the temperature (back to 25 °C, Fig. 11c) did not have any effect on the shoulder that stayed at 1019 cm^{-1}, but it appeared that the subsequent 1-butanol exposure led to its disappearance (Fig. 11d). This shift indicates that for $(NH_4)2PW$ the 1-butanol does penetrate the bulk and interact with H^+ and W═O_t.

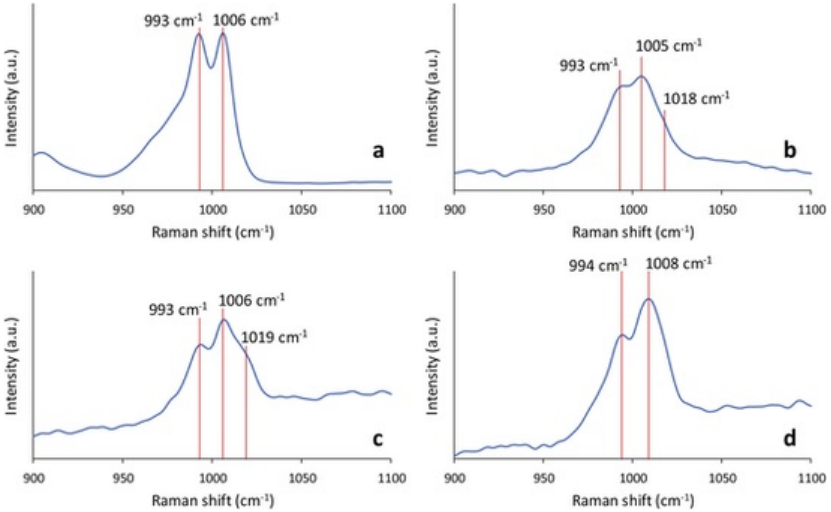

Fig. 11 Raman spectra of $(NH_4)2PW$ during the bulk activation procedure. a: At 25 °C under N_2, b: at 320 °C under N_2, c: back to 25 °C after thermal treatment under N_2, d: at 25 °C after thermal treatment under 1% 1-butanol in N_2.

Concerning *in situ* X-ray diffraction, the thermal treatment at 350 °C (Fig. 12) does not induce any modification in the crystalline phase that keeps its cubic centred symmetry. The fact that $(NH_4)2PW$ can only release a small amount of structural water when the temperature increases can explain this observation. Actually, NH_4^+ cations that are in the structure are not released with the temperature increase, which does not lead to any modification of the structure as it is the case when H_2O is released. Thus the cubic centred phase remains stable and almost unchanged thanks to the predominant presence of NH_4^+.

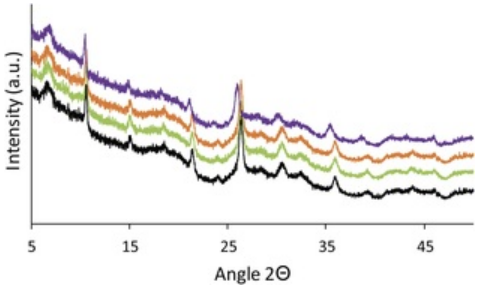

Fig. 12 Evolution of the XRD pattern of $(NH_4)2PW$ during the thermal treatment of the bulk activation procedure: – start 25 °C, – 350 °C, – 1 h 350 °C, – back to 25 °C.

1-Butanol exposure does not lead neither to any phase evolution (Fig. 13). Nevertheless, this does not mean that 1-butanol cannot penetrate the structure. It means that we cannot detect this event by XRD for the $(NH_4)2PW$ catalyst. The fact that the centred cubic structure is preserved despite the thermal treatment could play a role in 1-butanol penetration into the bulk, but it also prevents us from seeing its presence or absence in the bulk.

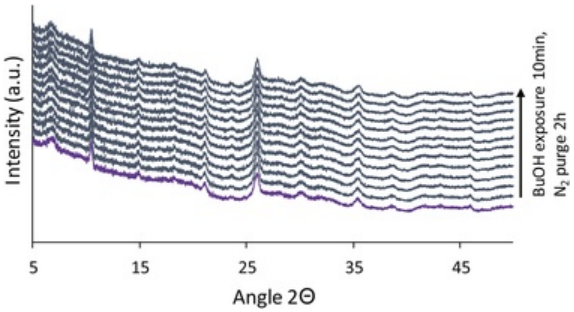

Fig. 13 Evolution of the XRD pattern of $(NH_4)2PW$ during 1-butanol exposure during the bulk activation procedure: – back to 25 °C (after thermal treatment), – BuOH exposure at 25 °C for 10 min and N_2 purge for 2 h.

In situ FT-IR shows that, as XRD, the thermal treatment and the subsequent 1-butanol exposure does not lead to any significant shift of the W O_t band in comparison with its original position at 980 cm^{-1} (Fig. 14). That means that under these conditions, it is not possible to pretend that 1-butanol has penetrated into the bulk. The other bands, as described before for H3PW, correspond to P–Oa–W (1080 cm^{-1}), W–Ob–W (893 cm^{-1}) and W–Oc–W (797 cm^{-1}).

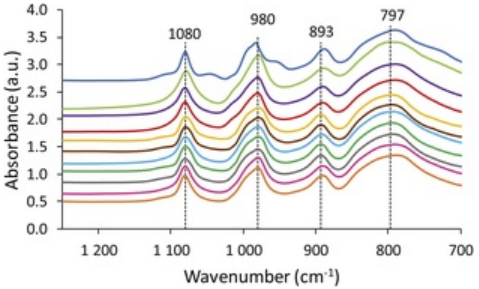

Fig. 14 Evolution of the IR spectrum of $(NH_4)2PW$ between 700 and 1200 cm^{-1} along the bulk activation procedure: – vacuum 29 °C, – vacuum 324 °C, – vacuum 123 °C, – BuOH 1.5 Torr 140 °C, – BuOH 1.5 Torr 19.5 °C, – BuOH 1.5 Torr 19.5 °C overnight, – BuOH 1.5 Torr 140 °C, – BuOH 1.5 Torr 22 °C, – vacuum 22 °C, – vacuum 123 °C, – vacuum 25 °C.

In the IR spectra between 1200 and 1800 cm^{-1} (Fig. 15) the band at 1420 cm^{-1} that is characteristic of ammonium ions is observed. The absence of the $H_5O_2^+$ band at 1700 cm^{-1} confirms the absence of crystallisation water as highlighted before and allows hypothesizing the more hydrophobic nature of the bulk of the catalyst. However, a band at 1620 cm^{-1} due to physisorbed water appears. Although their band decreased drastically, there are still some NH_4^+ present after the thermal treatment. So we are in a position allowing looking at the effect of the presence of NH_4^+ in the bulk (combined with the absence of structural water) on the ability of 1-butanol to penetrate the matrix of $(NH_4)2PW$.

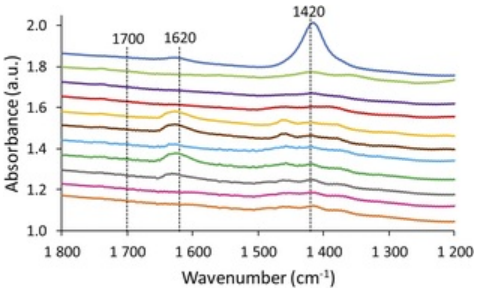

Fig. 15 Evolution of the IR spectrum of $(NH_4)2PW$ between 1200 and 1800 cm^{-1} along the bulk activation procedure: – vacuum 29 °C, – vacuum 324 °C, – vacuum 123 °C, – BuOH 1.5 Torr 140 °C, – BuOH 1.5 Torr 19.5 °C, – BuOH 1.5 Torr 19.5 °C overnight, – BuOH 1.5 Torr 140 °C, – BuOH 1.5 Torr 22 °C, – vacuum 22 °C, – vacuum 123 °C, – vacuum 25 °C.

In the 4000 to 2500 cm^{-1} zone (Fig. 16) the bands between 2800 and 3000 cm^{-1} (stretching of CH_3 from the 1-butanol in the gas phase and adsorbed at the surface) are again observed as, between 3100 and 3600 cm^{-1}, some large bands that correspond to OH stretching of 1-butanol and remaining water traces. Interestingly, after 1-butanol exposure at 25 °C, new well defined and intense bands appear at 3588 and 3532 cm^{-1}. These were neither present beforehand in the sequence, nor observed for H3PW. These bands are less intense but still present after heating at 150 °C under 1-butanol. This is exactly what we were expecting when applying the bulk activation procedure. Namely, after the thermal treatment is applied to remove water, the 1-butanol exposure at 25 °C leads to its penetration into the bulk. Thereby the bulk of the catalyst is accessible to 1-butanol even at higher temperature during the catalytic activity. These results confirm what was understood from *in situ* Raman, namely that the bulk can be activated thanks to the presence of NH_4^+ cations in the structure. The bands at 3588 and 3532 cm^{-1} are attributed to 1-butanol confined in the bulk, further confirming that it has penetrated the bulk and that the bulk has been activated.

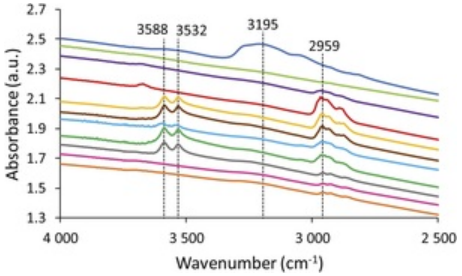

Fig. 16 Evolution of the IR spectrum of $(NH_4)2PW$ between 2500 and 4000 cm^{-1} during the bulk activation procedure: – vacuum 29 °C, – vacuum 324 °C, – vacuum 123 °C, – BuOH 1.5 Torr 140 °C, – BuOH 1.5 Torr 19.5 °C, – BuOH 1.5 Torr 19.5 °C overnight, – BuOH 1.5 Torr 140 °C, – BuOH 1.5 Torr 22 °C, – vacuum 22 °C, – vacuum 123 °C, – vacuum 25 °C.

3.2.3. $(NH_4)2.5PW$

In the case of $(NH_4)2.5PW$, the thermal treatment does not lead to any visible modification of the position of the W═O_t band, as 1-butanol exposure does not lead to any shift either (see ESI† Fig SI2). The band of W═O_t groups in interaction with the remaining H^+ is probably too low and is hidden by the band (not shifted) of the W═O_t groups in interaction with NH_4^+. Even if a small part of the W═O_t band shifted due to H^+ dehydration, it is not observed in the spectrum. This suggests that there is no bulk activation occurring for $(NH_4)2.5PW$, or that this phenomenon is not intense enough to be observed by *in situ* Raman spectroscopy.

3.3. Catalytic activity

Comparing H3PW with BuOH exposure, $(NH_4)2PW$ with BuOH exposure and $(NH_4)2.5PW$ with BuOH exposure (Fig. 17), $(NH_4)2.5PW$ appears the least active. This can be due to the weakness of its acid sites as revealed by NH_3-chemisorption (if the hypothesis that the ammonia release at low temperature in the experiment reflects the presence of weak acid sites indeed prevails), as compared to the superacidity of the other catalysts sites. The very low number of remaining protons in $(NH_4)2.5PW$ (revealed by *in situ* Raman) is so low that the effect of the bulk activation procedure is not distinguishable, which does also correlate with its lowest activity.

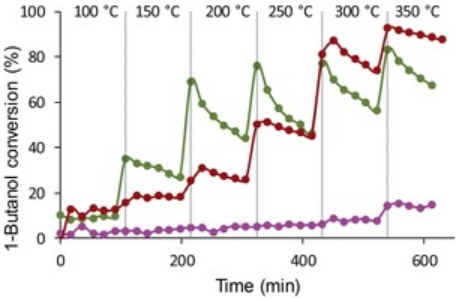

Fig. 17 Absolute catalytic activity of • $(NH_4)2PW$ BuOH exposure, compared to those of • $(NH_4)2.5PW$ BuOH exposure and • H3PW BuOH exposure.

For $(NH_4)2PW$ with BuOH exposure and H3PW with BuOH exposure the activity is not stable with the reaction time at each temperature explored above 100 °C, suggesting the occurrence of some kind of deactivation. A part of this deactivation can be explained by coke formation which increased with the temperature (carbon balance is shown in the ESI†). This phenomenon is more important in the case of $(NH_4)2PW$ with BuOH exposure. Another explanation could be that the water generated in the bulk of $(NH_4)2PW$ during the 1-butanol dehydration could clutter the spaces in the bulk, limiting the access of 1-butanol to the bulk, and thus decreasing the activity. The presence of water generated by the reaction can also increase the hydrophilicity of the structure and thereby decrease its interaction with 1-butanol and thus the ability of the latter to reach the protons inside the solid.

However, comparing $(NH_4)2PW$ with BuOH exposure and $(NH_4)2PW$ without BuOH exposure (Fig. 18), it turns out that the exposure step has a markedly beneficial effect on the activity. This is in good agreement with the *in situ* characterization that highlighted the possibility to activate the bulk of $(NH_4)2PW$. Here it is made clear that when 1-butanol has access to H^+ in the bulk as a result of a suitable activation procedure, the activity increases. For comparison, the gain in 1-butanol conversion is not so important at each temperature explored with H3PW with *vs.* without 1-butanol exposure (see ESI,† Fig. SI3), in agreement with what was observed during *in situ* characterization, namely that the applied activation procedure does not allow 1-butanol to penetrate in the bulk of H3PW.

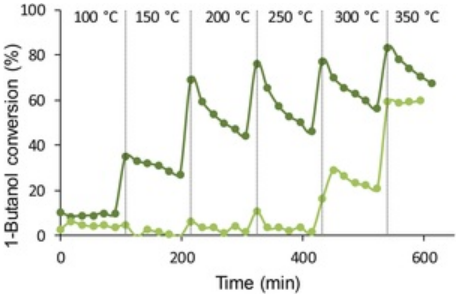

Fig. 18 Catalytic activity of • $(NH_4)2PW$ BuOH exposure compared to • $(NH_4)2PW$ no exposure.

To push the discussion towards a more quantitative level, the fact that the number of acid sites in the reactor is very different from one catalyst to another must be considered. Therefore, it is necessary to compare the activity of the different samples at an identical number of acid sites tested. On that purpose, Fig. 19 compares the activities normalized to the total number of acid sites in the reactor. Doing so the activity of $(NH_4)2PW$ appears much higher than that of H3PW, confirming that in the $(NH_4)2PW$ case the acid sites are more accessible for 1-butanol as a result of its bulk activation which boosts its performance.

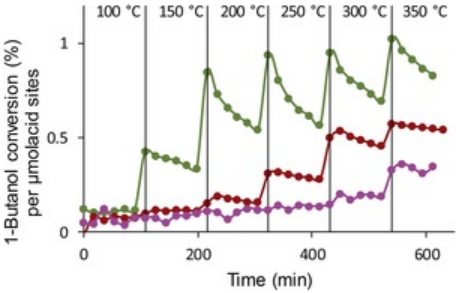

Fig. 19 Catalytic activity of • H3PW BuOH exposure, • $(NH_4)2PW$ BuOH exposure and • $(NH_4)2.5PW$ BuOH exposure, after normalization to the number of acid sites.

Finally, to discard all doubts that the observed gain of performance could be due to a textural effect induced by the activation of the bulk procedure, N_2 physisorption measurements were performed on fresh degassed samples, thermally treated ones, and on samples after BuOH exposure (see ESI,† Fig. SI4). In all cases, the specific surface area remains equally low and can thus not be invoked to account for the difference of performance from one sample to another.

The selectivities toward butenes and dibutylether are similar for all the catalysts regardless of their *x* value. At low temperature, dibutylether is favoured, and when increasing the temperature, butenes are more and more favoured. The condensation of 1-butanol to dibutylether is an exothermic equilibrated reaction, while the dehydration of 1-butanol to butene, or the dissociation of dibutylether to butenes is an endothermic irreversible reaction.[6] According to Le Chatelier's principle, we instinctively understand the selectivity towards dibutylether at low temperature (exothermic reaction, easy at low temperature), and the selectivity toward butenes at higher temperature (endothermic reaction that takes place thanks to the higher temperature, irreversible reaction). Selectivities of the different catalysts are discussed in more detail in the ESI† (Fig. SI5).

Concerning the carbon balance, it decreases when the temperature increases, indicating more coke formation at higher temperature. The bulk activation procedure also plays a role in decreasing the carbon balance, as it was previously described for other catalysts in methanol dehydration after bulk activation.[31] This phenomenon and the carbon balance of the catalysts are discussed in the ESI† (Fig. SI6). The deactivation of the catalysts by the formation of coke, and specifically of $(NH_4)2PW$ having undergone the bulk activation procedure, might be an obstacle for the industrial application of such systems. Indeed the regeneration of the catalysts by burning the coke at high temperature would not be appropriate due to their limited resistance to high temperature (our substituted ammonium HPAs decompose around 500 °C). The advantage of the partially substituted ammonium HPA salts and of our procedure to activate their bulk must thus be seen in the fact that they allow catalysis of the dehydration of 1-butanol at very low temperatures at which the carbon balance is very good, *i.e.* at which only dibutylether is produced with almost no (150 °C) or absolutely no coke formed, meaning that the deactivation is limited to its lowest expression (if it occurs).

4. Conclusion

The large size of 1-butanol and its hydrophobicity make its dehydration on HPA through a bulk pseudo liquid-type mechanism difficult, unlike what was observed with methanol. In this context we showed that the homogeneous replacement of some protons of $H_3PW_{12}O_{40}$ with NH_4^+ to form $(NH_4)_xH_{3-x}PW_{12}O_{40}$ leads to conservation of the crystalline structure of the material whilst a large amount of structural water was removed. Also ammonia-TPD shows that the modified Keggin salts still present some acidity (in terms of the number of acid sites), revealing that we succeeded in achieving the targeted only partial replacement of the protons with ammonium. In addition, for some catalysts these remaining protons still present strong acidity. Preserving numerous and strong acid sites was crucial for the targeted dehydration reaction. *In situ* characterization upon dehydration and subsequent 1-butanol exposure reveals that it is possible to activate the bulk (*i.e.* that this sequence allows 1-butanol to infiltrate the matrix of the solid) for $(NH_4)_2HPW_{12}O_{40}$, but not for H3PW. The conversion of 1-butanol achieved with this $(NH_4)_2HPW_{12}O_{40}$ modified catalyst thus outcompetes that of pristine $H_3PW_{12}O_{40}$. As initially hypothesized, the homogeneous distribution of ammonium as species substituting the protons within the solid helps 1-butanol to access every single proton still present in the catalyst, and ultimately increases significantly the activity for 1-butanol dehydration in butenes and dibutylether.

Conflicts of interest

Acknowledgements

The authors acknowledge the European Regional Development Fund (ERDF) and Wallonia (Operational Program “Wallonia-2020.EU”). Professor Marco Daturi (Normandie Université, ENSICAEN, UNICAEN, CNRS, Laboratoire Catalyse et Spectrochimie, Caen, France), supervisor of JS during her post-doctoral stay in his team, is acknowledged for letting her manage this collaboration in full autonomy and for letting her validate the Py-IR content of the manuscript.

References

1 D. Zhang, S. A. I. Barri and D. Chadwick, n-Butanol to iso-butene in one-step over zeolite catalysts, *Appl. Catal., A,* 2011, **403** (1–2), 1–11.

2 J. Schnee and E. M. Gaigneaux, Elucidating and exploiting the chemistry of Keggin heteropolyacids in the methanol-to-DME conversion: enabling the bulk reaction thanks to operando Raman, *Catal. Sci. Technol.,* 2017, **7** (4), 817–830.

3 J. Schnee, A. Eggermont and E. M. Gaigneaux, Boron nitride: a support for highly active heteropolyacids in the methanol-to-DME reaction, *ACS Catal.,* 2017, **7** (6), 4011–4017.

4 H. Knözinger, Dehydration of Alcohols on Alumina Oxide, *Angew. Chem., Int. Ed. Engl.,* 1968, **7** (10), 791–806.

5 A. M. Makarova, E. A. Paukshtis, J. M. Thomas, C. Williams and K. I. Zamaraev, Dehydration of n-Butanol on Zeolite H-ZSM5 and Amorphous Aluminosilicates : Detailed Mechanistic Study and the Effect of Pore Confinment, *J. Catal.,* 1994, **149** (1), 36–51.

6 Y. Khan, M. Marin, R. Karinen, J. Lehtonen and J. Kanervo, 1-Butanol dehydration in microchannel reactor: Kinetics and reactor modeling, *Chem. Eng. Sci.,* 2015, **137** (1), 740–751.

7 A. M. Varvarin, K. M. Khomenko and V. V. Brei, Conversion of n-butanol to hydrocarbons over H-ZSM-5, H-ZSM-11, H-L and H-Y zeolites, *Fuel,* 2013, **106,** 617–620.

8 J. H. Choi, J. K. Kim, D. R. Park, S. Park, J. Yi and I. K. Song, Etherification of n-butanol to di-n-butyl ether over $H_3PMo_{12-x}WxO_{40}$ (x=0, 3, 6, 9, 12) Keggin and $H_6P_2Mo_{18-x}W_xO_{62}$ (x=0, 3, 9, 15, 18) Wells–Dawson heteropolyacid catalysts, *Catal. Commun.,* 2011, **14** (1), 48–51.

9 I. V. Kozhevnikov, Sustainable heterogeneous acid catalysis by heteropoly acids, *J. Mol. Catal.,* 2007, **262** (1–2), 86–92.

10 M. J. Janik, J. Macht, E. Iglesia and M. Neurock, Correlating Acid Properties and Catalytic Function : A First-Principles Analysis of Alcohol Dehydration Pathways on Polyoxometalates Correlating Acid Properties and Catalytic Function : A First-Principles Analysis of Alcohol Dehydration Pathways on Polyox, *J. Phys. Chem. C,* 2009, **113** (5), 1872–1885.

11 I. V. Kozhevnikov, Catalysis by heteropoly acids and multicomponent polyoxometalates in liquid-phase reactions, *Chem. Rev.,* 1998, **98** (1), 171–198.

12 M. Misono, Heterogeneous Catalysis by Heteropoly Compounds of Molybdenum and Tungsten, *Catal. Rev.: Sci. Eng.,* 1987, **29** (2–3), 269–321.

13 J. Arichi, M. M. Pereira, P. M. Esteves and B. Louis, Synthesis of Keggin-type polyoxometalate crystals, *Solid State Sci.,* 2010, **12** (11), 1866–1869.

14 P. Putaj, Applications des polyoxométalates en catalyse hétérogène, PhD thesis, Université Claude Bernard Lyon I, Lyon, France, 2012.

15 M. J. Janik, K. A. Campbell, B. B. Bardin, R. J. Davis and M. Neurock, A computational and experimental study of anhydrous phosphotungstic acid and its interaction with water molecules, *Appl. Catal., A,* 2003, **256** (1–2), 51–68.

16 T. Okuhara, N. Mizuno and M. Misono, Catalytic Chemistry of Heteropoly Compounds, *Adv. Catal.,* 1996, **41,** 113–252.

17 M. Misono, Unique acid catalysis of heteropoly compounds (heteropolyoxometalates) in the solid state, *Chem. Commun.,* 2001, (13), 1141–1152.

18 J. Schnee and E. M. Gaigneaux, *Operando* Raman to Enhance the Methanol-to-DME Conversion Over Non-Thermally-Pretreated Keggin Heteropolyacids, *J. Phys. Chem. C,* 2017, **121** (1), 556–566.

19 T. Okuhara, T. Shin, K. Y. Lee and M. Misono, Catalysis by heteropolycompounds, absorption properties of 12tungstophosphoric acid and its salts, *Bull. Chem. Soc. Jpn.,* 1989, **62** (3), 717–723.

20 P. Vazquez, L. Pizzio, C. Caceres, M. Blanco, H. Thomas, E. Alesso, Ĺ. Finkielszteib, B. Lantano, G. Moltrasio and J. Aguirre, Silica-supported heteropolyacids as catalysts in alcohol dehydration reactions, *J. Mol. Catal. A: Chem.,* 2000, **161** (1–2), 223–232.

21 C. M. Prosser-McCartha, M. Kadkhodayan, M. M. Williamson, D. A. Bouchard and C. L. Hill, Photochemistry, spectroscopy, and X-ray structure of an intermolecular charge-transfer complex between an organic substrate and a polyoxometallate, α-$H_3PMo_{12}O_{40}$·6(tetramethylurea), *J. Chem. Soc., Chem. Commun.,* 1986, (24), 1747–1748.

22 L. Vegard, Die Konstitution der Mischkristalle une die Raumfüllung der Atome, *Z. Phys.,* 1921, **5,** 17–26.

23 T. Ito, K. Inumaru and M. Misono, Structure of Porous Aggregates of the Ammonium Salt of Dodecatungstophosphoric Acid, $(NH_4)_3PW_{12}O_{40}$: Unidirectionally Oriented Self-Assembly of Nanocrystallites, *J. Phys. Chem. B,* 1997, **101** (48), 9958–9963.

24 K. Okamoto, S. Uchida, T. Ito and N. Mizuno, Self-organization of all-inorganic dodecatungstophosphate nanocrystallites, *J. Am. Chem. Soc.,* 2007, **129** (23), 7378–7384.

25 J. Schnee and E. M. Gaigneaux, Raman monitoring of a catalytic system at work: Influence of the reactant on the sensitivity to laser-induced heating, *Spectrochim. Acta, Part A,* 2017, **173,** 151–159.

26 http://www.icdd.com/.

27 H. William, *Handbook of Chemistry and Physics*, CRC Press.

28 A. Micek-Ilnicka, The role of water in the catalysis on solid heteropolyacids, *J. Mol. Catal. A: Chem.,* 2009, **308** (1–2), 1–14.

29 M. Misono and T. Okuhara, Solid superacid catalysts, *CHEMTECH,* 1993, **23,** 111–112.

30 N. Essayem, R. Frety, G. Coudurier and J. C. Vedrine, Ammonia adsorption–desorption over the strong solid acid catalyst $H_3PW_{12}O_{40}$ and its Cs^+ and NH_4^+ salts : Comparison with sulfated zirconia, *J. Chem. Soc., Faraday Trans.,* 1997, **93** (17), 3243–3248.

31 J. Schnee and E. M. Gaigneaux, Lifetime of the $H_aPW_{12}C_{40}$ heteropolyacid in the methanol-to-DME process: A question of pre-treatment, *Appl. Catal., A,* 2017, **538,** 174–180.